Int. J. Solids Structures Vol. 19, No. 8, pp. 709–724, 1983
Printed in Great Britain.

0020-7683/83 $3.00 + .00
Pergamon Press Ltd.

LARGE STRAIN INELASTIC BEHAVIOUR OF CYLINDRICAL TUBES

E. CHATER and K. W. NEALE
Faculté des Sciences Appliquées, Université de Sherbrooke, Sherbrooke, Québec, Canada JIK 2R1

(*Received* 16 *June* 1982; *in revised form* 9 *December* 1982)

Abstract—The finite strain behaviour of thin-walled circular cylinders fixed at their ends and subjected to uniform internal pressure is examined. General transversely isotropic inelastic properties are assumed, and both time-independent plastic (elastoplastic) and rate-sensitive inelastic (viscoplastic) material response are considered. Flow theory and deformation theory-type constitutive laws are employed. The influence of constitutive properties and tube geometry on maximum pressure and localized necking instabilities is determined through finite element computations for selected types of anisotropy. Simple relations are developed for the pressure-deformation response and instability of general transversely isotropic materials, and these are shown to be very accurate for long tubes. The accuracy of elementary formulae commonly used in experimental investigations of constitutive relations is also discussed.

1. INTRODUCTION

Experimental investigations on material constitutive relationships are often carried out by subjecting thin-walled cylinders to various combinations of axial load and lateral pressure. In the treatment of test data it is commonly assumed that the expansion and elongation of the tube are uniform, so that simple expressions relating stress and strain components to the applied loads and displacements can be employed. One of the objectives of the present study is to examine some of the limitations of this approximation.

Instabilities in ductile cylindrical tubes are often associated with the state where the pressure or load reaches a maximum. Under load-controlled conditions the maximum pressure state does indeed lead to failure. However, if the displacements are controlled rather than the loads, failure generally occurs under decreasing pressure and at deformation levels which can exceed considerably the deformations at maximum pressure. For ductile materials, the mode of failure usually involves the development of a localized neck in some region of the tube. This neck eventually leads to fracture. In this investigation, the influence of material properties on maximum-pressure and localized-necking instabilities is determined.

The inelastic behaviour of pressurized cylinders has been the subject of many theoretical and experimental studies (see, e.g., Refs. [1–5]). An analytical investigation of the finite inelastic deformation of fixed-end circular tubes subject to internal pressure is carried out in this paper. Various constitutive laws describing anisotropic inelastic behaviour and either time-independent or strain-rate sensitive material response are incorporated in the analysis. The rate-dependent constitutive relations employed are viscoplastic generalizations of the well-known flow theory and deformation theory laws of time-independent plasticity. To characterize plastic anisotropy, we use the yield functions which have been proposed by Hill[6, 7], Bassani[8] and Budiansky[9] for transversely isotropic materials. The effects of the various constitutive parameters on the overall deformation behaviour of the tube is studied. The influence of cylinder geometry is also examined.

Numerical results are first obtained by finite element solutions based on Hill's extremum principle[10] for time-independent behaviour and a modified form of this principle[11] for viscoplastic materials. An approximate analysis is also proposed for long tubes. This analysis, which is based on the assumption of a uniform tube expansion, provides simple expressions for the pressure-deformation response as well as for the pressures and deformations at the maximum-pressure and localized-necking states. The approximate analysis is shown to agree extremely well with the finite element results. The simple relations given here are for general transversely isotropic materials and should therefore be quite useful for

assessing the influence of strain-hardening, strain-rate sensitivity and anisotropy on the large strain inelastic behaviour of cylindrical tubes.

2. BASIC FIELD EQUATIONS

A Lagrangian formulation of the basic field equations is adopted[12]. The initial undeformed configuration of the body, with volume V and surface S, is used as a reference. Material points are identified by convected coordinates x^i in this reference state. The covariant components of the metric tensors of the undeformed and deformed configurations are g_{ij} and G_{ij}, respectively. We denote the Lagrangian strain tensor by

$$\eta_{ij} = \frac{1}{2}(G_{ij} - g_{ij}) = \frac{1}{2}(u_{i,j} + u_{j,i} + u^k_{,i}u_{k,j}) \tag{2.1}$$

where u_i are the components of the displacement vector on the reference base vectors $\mathbf{g}^i$ and a comma represents covariant differentiation with respect to the undeformed metric. The Lagrangian strain-rate components are

$$\dot{\eta}_{ij} = \frac{1}{2}(\dot{u}_{i,j} + \dot{u}_{j,i} + u^k_{,i}\dot{u}_{k,j} + \dot{u}^k_{,i}u_{k,j}) \tag{2.2}$$

where a superposed dot denotes differentiation with respect to time.

Another strain measure employed in this analysis is the logarithmic strain tensor which, by definition, is coaxial with the Lagrangian strain ellipsoid and has principal values ϵ_i. The ϵ_i are related to the principal components of η_{ij} as follows

$$\epsilon_i = \ln \lambda_i = \frac{1}{2}\ln(2\eta_i + 1) \tag{2.3}$$

where λ_i are the principal stretches. For incompressible deformations, the constraint $\lambda_1\lambda_2\lambda_3 = 1$ implies the simple condition $\epsilon_1 + \epsilon_2 + \epsilon_3 = 0$.

We first consider time-independent materials with constitutive laws of the form

$$\overset{\nabla}{\tau}{}^{ij} = L^{ijkl}\dot{\eta}_{kl} \tag{2.4}$$

where L^{ijkl} denotes the tensor of instantaneous moduli and $\overset{\nabla}{\tau}{}^{ij}$ are the Jaumann rates of the Kirchhoff stress tensor τ. The contravariant components τ^{ij} are defined with respect to the deformed base vectors $\mathbf{G}_i$ and are related to the Cauchy stress components σ^{ij} by

$$\tau^{ij} = \frac{\rho_0}{\rho}\sigma^{ij} \tag{2.5}$$

where ρ_0 and ρ are the densities in the initial and current states, respectively. The tensor $\mathbf{L}$ is assumed to have the symmetry properties ($i \longleftrightarrow j$, $k \longleftrightarrow l$, $ij \longleftrightarrow kl$) required for the existence of potential functions for $\overset{\nabla}{\tau}{}^{ij}$. That is, the constitutive law (2.4) can alternatively be expressed as follows

$$\overset{\nabla}{\tau}{}^{ij} = \frac{\partial U}{\partial \dot{\eta}_{ij}} \tag{2.6}$$

with

$$U(\dot{\eta}) = \frac{1}{2}L^{ijkl}\dot{\eta}_{ij}\dot{\eta}_{kl}. \tag{2.7}$$

Hill's extremum principle[10] for rate-independent elastoplastic solids states that the

incremental equilibrium behaviour of the body is governed by the following variational equation

$$\delta J = 0$$

with

$$J(u) = \int_V \left[U(\dot{\eta}) - G^{kl}\tau^{ij}\dot{\eta}_{li}\dot{\eta}_{kj} + \frac{1}{2}\tau^{ij}\dot{u}^k_{,i}\dot{u}_{k,j} \right] \mathrm{d}V - \int_{S_P} \Psi(\dot{u})\,\mathrm{d}S. \tag{2.8}$$

The admissible velocity fields here are assumed to satisfy the prescribed kinematic boundary conditions. In (2.8) S_P represents the part of the surface on which the nominal traction rates $\dot{\mathbf{F}}$ are prescribed and $\Psi(\dot{u})$ is the potential function for the $\dot{\mathbf{F}}$ such that

$$\delta\Psi(\dot{u}) = \dot{F}^i\delta\dot{u}_i \tag{2.9}$$

For a fluid pressure loading p applied to a surface element $\mathrm{d}S$ with unit outward normal $\mathbf{n} = n_i\mathbf{g}^i$ in the initial reference state, we have[13]

$$F_k = -p\epsilon_{ijk}\alpha^{ij} \tag{2.10}$$

where

$$\alpha^{ij} = \frac{1}{2}\epsilon^{pqr}n_r(\delta_p{}^i + u^i_{,p})(\delta_q{}^j + u^j_{,q}). \tag{2.11}$$

In (2.11), ϵ_{ijk} is the alternating tensor and δ_j^i is the Kronecker delta.

Strain-rate dependent behaviour is represented by an elastic–viscoplastic constitutive law. The strain-rate is decomposed as follows

$$\dot{\eta}_{ij} = \dot{\eta}'_{ij} + \dot{\eta}''_{ij} \tag{2.12}$$

where $\dot{\eta}'_{ij}$ is the instantaneous part or that which is a function of the stress rates $\overset{\nabla_{ij}}{\tau}$, and $\dot{\eta}''_{ij}$ denotes the part which does not depend explicitly on the rates $\overset{\nabla_{ij}}{\tau}$. Hill's functional (2.8) can be modified for viscoplastic behaviour by assuming the stress-rates $\overset{\nabla_{ij}}{\tau}$ to be derivable from a potential function of the *instantaneous* strain-rates $\dot{\eta}'_{ij} = \dot{\eta}_{ij} - \dot{\eta}''_{ij}$[11]. That is,

$$\overset{\nabla_{ij}}{\tau} = \frac{\partial U'}{\partial \dot{\eta}'_{ij}} \tag{2.13}$$

where

$$U'(\dot{\eta}') = \frac{1}{2}L^{ijkl'}(\dot{\eta}_{ij} - \dot{\eta}''_{ij})(\dot{\eta}_{kl} - \dot{\eta}''_{kl}) \tag{2.14}$$

and $\mathbf{L}'$ are the instantaneous moduli in the relation

$$\overset{\nabla_{ij}}{\tau} = L^{ijkl'}(\dot{\eta}_{ij} - \dot{\eta}''_{ij}). \tag{2.15}$$

In Hill's functional we now replace $U(\dot{\eta})$ by $U'(\dot{\eta}')$. In applying this modified variational principle we take $\delta\dot{\eta}''_{ij} = 0$ since the components $\dot{\eta}''_{ij}$ do not depend explicitly on stress rates.

3. CONSTITUTIVE RELATIONS

Incompressible materials with transversely isotropic inelastic properties are considered, with the thickness direction of a tube element being the axis of transverse isotropy. Since

the elastic response is expected to have a negligible influence on the large deformation behaviour of the tube, elastic anisotropy will be neglected.

For time-independent material response the total strain-rate is decomposed as follows

$$\dot{\epsilon}_i = \dot{\epsilon}_i^e + \dot{\epsilon}_i^p \tag{3.1}$$

where $\dot{\epsilon}_i^e$ is the elastic part and $\dot{\epsilon}_i^p$ denotes the plastic part. The elastic strain-rates are given by

$$\begin{aligned} \dot{\epsilon}_i^e &= \frac{1}{2E}[3\dot{\sigma}_i - (\dot{\sigma}_1 + \dot{\sigma}_2)] \quad i = 1, 2 \\ \dot{\epsilon}_3^e &= -(\dot{\epsilon}_1^e + \dot{\epsilon}_2^e). \end{aligned} \tag{3.2}$$

Here E is the elastic modulus and $\dot{\sigma}_i$ are the principal Cauchy stress-rates. Because of incompressibility the $\dot{\sigma}_i$ are equal to the principal Kirchhoff stress-rates $\dot{\tau}_i$. Since our analysis will be based on the usual assumptions of membrane theory we consider plane stress conditions with the stress in the thickness direction $\sigma_3 = 0$.

A general transversly isotropic yield function recently proposed by Budiansky[9] is used to derive the plastic strain-rates. Other yield criteria due to Bassani[8] and Hill[6, 7] are special cases of Budiansky's yield function. The following parametric form is proposed by Budiansky

$$\frac{\sigma_1 - \sigma_2}{2\sigma_s} = g(\phi)\sin\phi, \quad \frac{\sigma_1 + \sigma_2}{2\sigma_b} = g(\phi)\cos\phi \tag{3.3}$$

where, with $g(0) = g(\pm\pi/2) = 1$, σ_s and σ_b represent the current yield stresses in pure shear and equibiaxial tension, respectively. The equivalent uniaxial stress σ_u is given by

$$\sigma_u = 2\sigma_b g(\phi_u)\cos\phi_u \quad \text{with} \quad \phi_u = \tan^{-1}\left(\frac{\sigma_b}{\sigma_s}\right) \tag{3.4}$$

According to flow theory, the plastic strain-rates are as follows

$$\begin{aligned} \dot{\epsilon}_i^p &= \frac{\partial\sigma_u}{\partial\sigma_i}\dot{\epsilon}_u^p \quad i = 1, 2 \\ \dot{\epsilon}_3^p &= (\dot{\epsilon}_1^p + \dot{\epsilon}_2^p) \end{aligned} \tag{3.5}$$

where $\dot{\epsilon}_u^p$ is the effective strain-rate. The following relationship between $\dot{\epsilon}_u^p$ and $\dot{\sigma}_u$ is assumed

$$\dot{\epsilon}_u^p = \left(\frac{1}{E_t} - \frac{1}{E}\right)\dot{\sigma}_u \tag{3.6}$$

where the tangent modulus value $E_t(\sigma_u)$ is obtained from the uniaxial true stress–natural strain curve at the current stress level σ_u. The normality rule (3.5) together with the plastic work postulate $\mathrm{d}W^p = \sigma_i\dot{\epsilon}_i^p = \sigma_u\dot{\epsilon}_u^p$ gives[9]

$$\begin{aligned} \dot{\epsilon}_1^p &= \frac{\dot{\epsilon}_u^p}{2g^2}\left[-\left(\frac{Y}{X}\right)(g\cos\phi)' + \left(\frac{1}{X}\right)(g\sin\phi)'\right] \\ \dot{\epsilon}_2^p &= \frac{\dot{\epsilon}_u^p}{2g^2}\left[\left(\frac{Y}{X}\right)(g\cos\phi)' + \left(\frac{1}{X}\right)(g\sin\phi)'\right] \\ \dot{\epsilon}_3^p &= -(\dot{\epsilon}_1^p + \dot{\epsilon}_2^p) \end{aligned} \tag{3.7}$$

where $X = \sigma_b/\sigma_u$, $Y = \sigma_b/\sigma_s$ and a prime designates differentiation with respect to ϕ. Isotropic hardening is implied whenever the stress ratios X and Y are taken to be constant.

The finite-strain deformation theory equations corresponding to (3.5) are

$$\epsilon_i^p = \frac{\partial \sigma_u}{\partial \sigma_i} \epsilon_u^p \tag{3.8}$$

where the derivatives $\partial\sigma_u/\partial\sigma_i$ are as identified by (3.5) and (3.7). That is, we simply replace $\dot{\epsilon}_i^p$, $\dot{\epsilon}_u^p$ in (3.7) by their total (logarithmic) values ϵ_i^p, ϵ_u^p to obtain the deformation theory relations. Now the effective plastic strain ϵ_u^p is related to σ_u as follows

$$\epsilon_u^p = \left(\frac{1}{E_s} - \frac{1}{E}\right)\sigma_u \tag{3.9}$$

where the secant modulus $E_s(\sigma_u)$ is determined from the true stress–natural strain curve in simple tension.

The anisotropic yield function proposed by Bassani[8] is obtained with the following choice for $g(\phi)$

$$(g \sin\phi)^m + (g \cos\phi)^n = 1 \tag{3.10}$$

An alternative form for (3.10) is

$$|\sigma_1 + \sigma_2|^n + \frac{n}{m}(1+2R)\,\sigma_u^{n-m}|\sigma_1 - \sigma_2|^m = \left[1 + \frac{n}{m}(1+2R)\right]\sigma_u^n \tag{3.11}$$

in which the parameter R represents the ratio $\dot{\epsilon}_2^p/\dot{\epsilon}_3^p$ for uniaxial tension in the 1-direction. Bassani's yield function (3.11) reduces to Hill's recent yield criterion[7] when $n = m$ and to Hill's original function when $n = m = 2$. The choice $n = m = 2$ and $R = 1$ in (3.11) implies isotropic behaviour.

A uniaxial stress–strain curve of the form

$$\sigma_u = \begin{cases} E\epsilon_u & \text{for} \quad \sigma_u \le \sigma_y \\ K\epsilon_u^N & \text{for} \quad \sigma_u \ge \sigma_y \end{cases} \tag{3.12}$$

is assumed in the computations for time-independent response. Here K is a constant, σ_y is the yield stress and N is the strain-hardening exponent. As the ratio E/K becomes large, (3.12) approaches rigid-plastic behaviour.

An elastic–viscoplastic generalization of the above laws is employed to model strain-rate sensitive material behaviour. The strain-rates are now comprised of an elastic part $\dot{\epsilon}_i^e$, again given by (3.2), plus a viscoplastic part $\dot{\epsilon}_i^{vP}$, i.e.

$$\dot{\epsilon}_i = \dot{\epsilon}_i^e + \dot{\epsilon}_i^{vP}. \tag{3.13}$$

By analogy with the flow theory relations (3–5) we take

$$\dot{\epsilon}_i^{vP} = \frac{\partial \sigma_u}{\partial \sigma_i} \dot{\epsilon}_u^{vP} \tag{3.14}$$

where $\dot{\epsilon}_u^{vP}$ is the effective viscoplastic strain-rate. The analogous viscoplastic "deformation theory" relations obtained by differentiating (3.8) are

$$\dot{\epsilon}_i^{vP} = \frac{\partial \sigma_u}{\partial \sigma_i} \dot{\epsilon}_u^{vP} + \epsilon_u^{vP} \frac{\partial^2 \sigma_u}{\partial \sigma_i \partial \sigma_k} \dot{\sigma}_k. \tag{3.15}$$

Strain-rate sensitivity is modelled through the uniaxial stress–strain–strain rate relation,

which is assumed to be of the form

$$\dot{\epsilon}_u^{vP} = \mathscr{G}(\sigma_u, \epsilon_u^{vP}). \tag{3.16}$$

In the decomposition (2.12) the time-dependent components become

$$\dot{\epsilon}_i'' = \mathscr{G} \frac{\partial \sigma_u}{\partial \sigma_i} \tag{3.17}$$

in both the flow theory and deformation theory versions. The instantaneous components are $\dot{\epsilon}_i' = \dot{\epsilon}_i^e$ with flow theory, whereas deformation theory gives

$$\dot{\epsilon}_i' = \dot{\epsilon}_i^e + \epsilon_u^{vP} \frac{\partial^2 \sigma_u}{\partial \sigma_i \partial \sigma_k} \dot{\sigma}_k. \tag{3.18}$$

As mentioned in [14, 15], the above rate-dependent deformation theory does not in general describe path-independent stress–strain behaviour. We shall, however, continue to refer to (3.15) as rate-sensitive "deformation theory" equations because of their connection with the path-independent relations (3.8) of time-independent deformation theory.

The function $\mathscr{G}(\sigma_u, \epsilon_u^{vP})$ is obtained using the following stress–strain–strain rate curve suggested by Wang and Wenner[16]

$$\sigma_u = \begin{cases} E\epsilon_u & \text{for } \sigma_u \leq \sigma_y \\ K\left[(\epsilon_u^{vP} + \epsilon_0)^N + \kappa \ln\left(1 + \dfrac{\dot{\epsilon}_u^{vP}}{\dot{\epsilon}_R}\right)\right] & \text{for } \sigma_u \geq \sigma_y. \end{cases} \tag{3.19}$$

Here ϵ_0 is a constant, κ is the strain-rate sensitivity index and $\dot{\epsilon}_R$ represents a reference strain-rate. When $\kappa = 0$ (3.19) describes time-independent plastic response.

4. GOVERNING RELATIONS FOR CIRCULAR TUBE

The general formulation of the previous sections will now be specialized to the problem of an incompressible axisymmetric circular tube fixed at its ends and subjected to a uniform internal pressure p (Fig. 1). The length, radius and thickness of the cylinder are $2l_0$, r_0 and h_0 initially and $2l_0$, r and h in the deformed state. We shall limit attention to thin-walled cylinders (r_0/h_0, $l_0/h_0 \gg 1$) and adopt the usual assumptions of membrane theory.

A cylindrical polar coordinate system is used as a reference with $x^1 \equiv z$, $x^2 \equiv \theta$ and $x^3 \equiv r$ (Fig. 1). The undeformed metric tensor has components

$$g_{zz} = g^{zz} = 1, \quad g_{\theta\theta} = 1/g^{\theta\theta} = r_0^2, \quad g_{rr} = g^{rr} = 1. \tag{4.1}$$

Because of symmetry and the membrane theory approximations, the mid-surface displacement components become

$$u_z = u^z = u(z), \quad u_\theta = u^\theta = 0, \quad u_r = u^r = w(z). \tag{4.2}$$

From (2.1) and (2.3) we obtain the following for the logarithmic strain components

$$\begin{aligned} \epsilon_z &= \ln \lambda_z = \ln \{[(1 + u_{,z})^2 + w_{,z}^2]^{1/2}\} \\ \epsilon_\theta &= \ln \lambda_\theta = \ln\left(1 + \frac{w}{r_0}\right) \\ \epsilon_h &= \ln \lambda_h = \ln\left(\frac{h}{h_0}\right) \end{aligned} \tag{4.3}$$

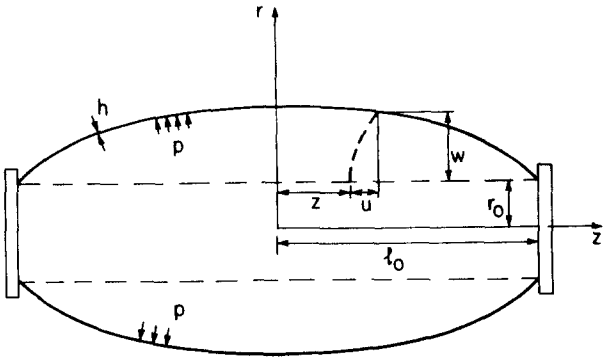

Fig. 1. Fixed-end circular tube under internal pressure.

where a comma now denotes differentiation with respect to z. Because of incompressibility $\epsilon_h = -(\epsilon_z + \epsilon_\theta)$ and $\lambda_h = (\lambda_z\lambda_\theta)^{-1}$. The deformed metric has the following components

$$G_{zz} = \frac{1}{G^{zz}} = \lambda_z^2, \quad G_{\theta\theta} = \frac{1}{G^{\theta\theta}} = (r_0\lambda_\theta)^2, \quad G_{rr} = G^{rr} = \lambda_h^2. \tag{4.4}$$

The strain-rate components corresponding to (4.3) are $\dot{\epsilon}_z = \dot{\lambda}_z/\lambda_z$, etc. They are related to the Lagrangian strain-rates (2.2) as follows

$$\dot{\eta}_{zz} = \lambda_z^2\dot{\epsilon}_z, \quad \dot{\eta}_{\theta\theta} = (r_0\lambda_\theta)^2\dot{\epsilon}_\theta. \tag{4.5}$$

The nominal traction components for the configuration-dependent pressure loading are obtained using (2.10) and (2.11). We get

$$\begin{aligned} F_z &= F^z = -p\left(1 + \frac{w}{r_0}\right) w_{,z} \\ F_\theta &= F^\theta = 0 \\ F_r &= F^r = p\left(1 + \frac{w}{r_0}\right)\left(1 + u_{,z}\right). \end{aligned} \tag{4.6}$$

Applying (2.9) gives the following for the traction-rate potential Ψ

$$\psi = \left[-\dot{p}\left(1 + \frac{w}{r_0}\right) w_{,z} - p\dot{w}_{,z}\right]\dot{u} + \left\{\dot{p}\left(1 + \frac{w}{r_0}\right)(1 + u_{,z}) + p\left[\frac{w}{r_0}\dot{u}_{,z} + \frac{1}{2}(1 + u_{,z})\frac{\dot{w}}{r_0}\right]\right\}\dot{w}. \tag{4.7}$$

Because of symmetry and incompressibility the only non-zero membrane stresses are $\tau^{zz} = \sigma^{zz}(z)$ and $\tau^{\theta\theta} = \sigma^{\theta\theta}(z)$. They are related to the principal Cauchy stresses as follows

$$\sigma_z = \lambda_z^2\sigma^{zz}, \quad \sigma_\theta = (r_0\lambda_\theta)^2\sigma^{\theta\theta}. \tag{4.8}$$

For time-independent material behaviour, the constitutive laws presented in the previous section take the form

$$\begin{aligned} \dot{\epsilon}_z &= M_{zz}\dot{\sigma}_z + M_{z\theta}\dot{\sigma}_\theta \\ \dot{\epsilon}_\theta &= M_{z\theta}\dot{\sigma}_z + M_{\theta\theta}\dot{\sigma}_\theta. \end{aligned} \tag{4.9}$$

Expressions for the instantaneous compliances $\mathbf{M}$ according to flow theory (3.5) and deformation theory (3.8) are given in the Appendix. Equations (4.9) can be inverted to give

$$\dot{\sigma}_z = L_{zz}\dot{\epsilon}_z + L_{z\theta}\dot{\epsilon}_\theta$$
$$\dot{\sigma}_\theta = L_{z\theta}\dot{\epsilon}_z + L_{\theta\theta}\dot{\epsilon}_\theta \tag{4.10}$$

where the instantaneous moduli $\mathbf{L} = \mathbf{M}^{-1}$.

The constitutive relations for strain-rate dependent behaviour can be expressed as follows

$$\dot{\epsilon}_z = (M'_{zz}\dot{\sigma}_z + M'_{z\theta}\dot{\sigma}_\theta) + \dot{\epsilon}''_z$$
$$\dot{\epsilon}_\theta = (M'_{z\theta}\dot{\sigma}_z + M'_{\theta\theta}\dot{\sigma}_\theta) + \dot{\epsilon}''_\theta \tag{4.11}$$

where $\dot{\epsilon}''_z$, $\dot{\epsilon}''_\theta$ are as given by (3.17). Inverting (4.11) gives

$$\dot{\sigma}_z = L'_{zz}(\dot{\epsilon}_z - \dot{\epsilon}''_z) + L'_{z\theta}(\dot{\epsilon}_\theta - \dot{\epsilon}''_\theta)$$
$$\dot{\sigma}_\theta = L'_{z\theta}(\dot{\epsilon}_z - \dot{\epsilon}''_z) + L'_{\theta\theta}(\dot{\epsilon}_\theta - \dot{\epsilon}''_\theta) \tag{4.12}$$

with $\mathbf{L}' = (\mathbf{M}')^{-1}$. Expressions for the $\mathbf{M}'$ as determined from the rate-dependent flow theory and deformation theory laws of the previous sections are given in the Appendix.

In view of the above relations the functional (2.8) for time-independent behaviour becomes

$$J = 2\pi r_0 \int_0^{l_0} \left\{ h_0 \left[U(\dot{\epsilon}) - \sigma_z \dot{\epsilon}_z^2 - \sigma_\theta \dot{\epsilon}_\theta^2 + \frac{\sigma_z}{2\lambda_z^2}(\dot{u}_{,z}^2 + \dot{w}_{,z}^2) + \frac{\sigma_\theta}{2\lambda_\theta^2}\left(\frac{\dot{w}}{r_0}\right)^2 - \Psi \right\} \mathrm{d}z \tag{4.13}$$

with

$$U(\dot{\epsilon}) = \frac{1}{2} L_{zz}\dot{\epsilon}_z^2 + L_{z\theta}\dot{\epsilon}_z\dot{\epsilon}_\theta + \frac{1}{2} L_{\theta\theta}\dot{\epsilon}_\theta^2. \tag{4.14}$$

The corresponding functional for rate-sensitive behaviour is obtained by replacing $U(\dot{\epsilon})$ in (4.13) by

$$U'(\dot{\epsilon}') = \frac{1}{2} L'_{zz}(\dot{\epsilon}_z - \dot{\epsilon}''_z)^2 + L'_{z\theta}(\dot{\epsilon}_z - \dot{\epsilon}''_z)(\dot{\epsilon}_\theta - \dot{\epsilon}''_\theta) + \frac{1}{2} L'_{\theta\theta}(\dot{\epsilon}_\theta - \dot{\epsilon}''_\theta)^2. \tag{4.15}$$

For an applied pressure increment $\dot{p}$ the velocity fields are determined by the variational equation

$$\delta J(\dot{u}, \dot{w}) = 0. \tag{4.16}$$

Here the velocity fields are constrained to satisfy the following boundary conditions

$$\dot{u}(0) = \dot{w}_{,z}(0) = 0$$
$$\dot{u}(l_0) = \dot{w}(l_0) = 0. \tag{4.17}$$

As mentioned earlier, the components $\dot{\epsilon}''_z$, $\dot{\epsilon}''_\theta$ for rate-dependent response are assumed to be expressed in terms of the current state of stress and deformation through (3.17). Consequently we take $\delta\dot{\epsilon}''_z = \delta\dot{\epsilon}''_\theta = 0$ when applying (4.16). Finite element solutions for both time-independent and rate-dependent behaviour are developed using the above variational principles.

5. APPROXIMATE ANALYSIS FOR LONG TUBES

Approximate formulae for long tubes ($l_0/r_0 \gg 1$) can be obtained by neglecting end conditions and assuming a uniform expansion $w = w_0$ of the cylinder under plane strain conditions ($\epsilon_z = u = 0$). As a result

$$\epsilon_\theta = -\epsilon_h = \ln\left(1 + \frac{w_0}{r_0}\right) \tag{5.1}$$

and

$$\sigma_\theta = \frac{pr_0}{h_0}\left(1 + \frac{w_0}{r_0}\right)^2. \tag{5.2}$$

Since proportional loading is implied here, the predictions of flow theory and deformation theory of plasticity are identical.

We first consider time-independent behaviour and introduce the following (constant) stress ratios

$$\alpha = \frac{\sigma_z}{\sigma_\theta}, \quad \beta = \frac{\sigma_\theta}{\sigma_u}. \tag{5.3}$$

If elastic effects are neglected α and β can be determined for a given yield function $g(\phi)$ by solving (3.3) together with the condition $\dot{\epsilon}_1^P = 0$ in (3.7a). With Hill's recent criterion ($n = m$) the following explicit expressions are obtained for the stress ratios

$$\alpha = \frac{\gamma - 1}{\gamma + 1}, \quad \gamma = (1 + 2R)^{1/(n-1)}, \quad \beta = \left[\frac{2(1+R)}{(1+\alpha)^n + (1+2R)(1-\alpha)^n}\right]^{1/n}. \tag{5.4}$$

For a power-law hardening law of the form $\sigma_u = K\epsilon_u^N$, the pressure-expansion curve (for any transversely isotropic material) becomes

$$\frac{pr_0}{Kh_0} = \beta^{N+1}\left[\ln\left(1 + \frac{w_0}{r_0}\right)\right]^N\left(1 + \frac{w_0}{r_0}\right)^{-2}. \tag{5.5}$$

At the maximum pressure p^* we have

$$\begin{aligned} \epsilon_\theta^* &= \frac{N}{2} \\ \frac{w_0^*}{r_0} &= \exp\left(\frac{N}{2}\right) - 1 \\ \frac{p^* r_0}{Kh_0} &= \beta^{N+1}\left(\frac{N}{2}\right)^N \exp(-N). \end{aligned} \tag{5.6}$$

Localization, as determined from a necking-band bifurcation analysis (see [15]), occurs when

$$\begin{aligned} \epsilon_\theta^{(l)} &= N \\ \frac{w_0^{(l)}}{r_0} &= \exp(N) - 1 \\ \frac{p^{(l)} r_0}{Kh_0} &= \beta^{N+1}(N)^N \exp(-2N). \end{aligned} \tag{5.7}$$

The above relations indicate that localized necking occurs at expansion levels $w_0^{(l)}$ which are greater than those (w_0^*) at the maximum pressure. Furthermore, anisotropy has no influence on the deformation values w_0^*, $w_0^{(l)}$ at instability. Anisotropy does, however, affect the pressure values p_0^*, $p_0^{(l)}$ at the instability through the parameter β.

For strain-rate sensitive response we again neglect elastic effects and use the uniaxial law (3.19b) with $\epsilon_0 = 0$. The pressure-expansion relation becomes

$$\frac{pr_0}{Kh_0} = \beta\left(1 + \frac{w_0}{r_0}\right)^{-2}\left\{\beta^N\left[\ln\left(1 + \frac{w_0}{r_0}\right)\right]^N + \kappa \ln\left[1 + \frac{\beta \dot{w}_0}{\dot{\epsilon}_R(r_0 + w_0)}\right]\right\} \tag{5.8}$$

which reduces to the rate-independent result (5.5) when $\kappa = 0$ or when the applied expansion rate $\dot{w}_0$ approaches zero. For cases where the expansion strain-rate $\dot{\epsilon}_\theta$ is prescribed to be constant, the maximum pressure occurs at the following state

$$\beta^N \epsilon_\theta^N \left(\frac{N}{\epsilon_\theta} - 2\right) = 2\kappa \ln\left(1 + \frac{\beta \dot{\epsilon}_\theta}{\dot{\epsilon}_R}\right) \tag{5.9}$$

which, for small values of κ, is not too different from the rate-independent result (5.6). As discussed in [14], localized-necking bifurcations are excluded here since the material behaviour is strain-rate dependent.

The accuracy of the proposed simplified relations will be examined in the next section where we compare some finite element results to those obtained with the above analysis.

6. NUMERICAL RESULTS AND DISCUSSION

The numerical analysis of the fixed-end tube is carried out by incorporating a particular finite element scheme[17] in the variational equation (4.16). With this method quadratic shape functions are employed for the velocity fields $\dot{u}(z)$, $\dot{w}(z)$ within each element. Furthermore, continuity of the gradients $\dot{u}_{,z}$ and $\dot{w}_{,z}$ is imposed at the element boundaries by means of the Lagrange multiplier technique. Simpson's quadrature formula is used to compute the integrals in (4.13). A detailed description of the finite element technique is given in [17].

For rate-independent response, the pressure-expansion behaviour of the tube is obtained from a straightforward incremental solution of the finite element equations. To avoid numerical difficulties near the maximum pressure, the displacement increments $\Delta w(0) \equiv \Delta w_0$ were prescribed (rather than pressure increments Δp) and the corresponding pressure, displacement, strain and stress increments throughout the tube were computed. Between 100 and 150 increments were used to reach the maximum pressure state.

For strain-rate sensitive behaviour, an explicit time integration of the finite element equations was performed. A constant expansion rate $\dot{w}(0) \equiv \dot{w}_0$ was prescribed and the corresponding pressure, displacement and stress increments for each time-increment Δt were computed. To assure convergent and numerically stable solutions, the time-steps Δt were chosen in accordance with the convergence criterion developed in [11].

If we initially assume $\sigma_z = \sigma_\theta = u = w = 0$ throughout the tube the solution to (4.16) for the first increment becomes $\dot{u} = \dot{w} = 0$. Consequently, to start the computational procedure a uniform axial stress $\sigma_z = s_0$, with s_0 very small, was initially prescribed. We also considered initial conditions where small initial deflections of the tube were prescribed. Both types of initial condition led to essentially identical results provided that the initial stress or displacement values remained sufficiently small.

Numerical results for the pressurized tube are given in Figs. 1–4 and in Tables 1–4. A non-dimensional pressure

$$\bar{p} = \frac{pr_0}{Kh_0} \tag{6.1}$$

is introduced because, in terms of this quantity, the governing equations are independent of the initial radius-to-thickness ratio r_0/h_0 of the tube.

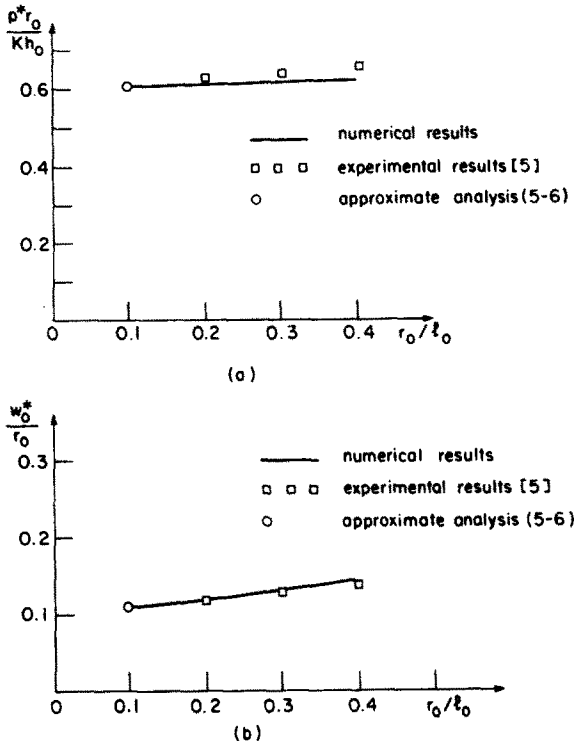

Fig. 2. Dependence of maximum pressure p^* and corresponding deflection w_0^* on diameter-to-length ratio of tube (time-independent behaviour).

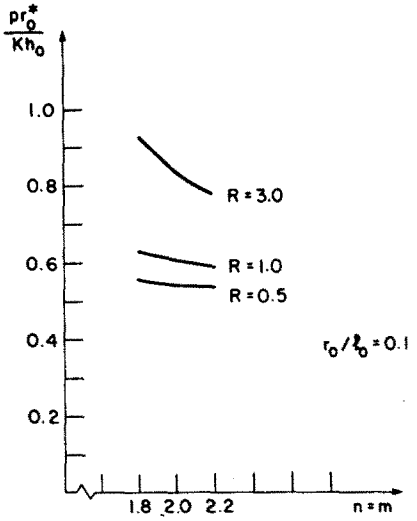

Fig. 3. Dependence of maximum pressure p^* on anisotropic parameters (time-independent behaviour).

The material constants assumed in the calculations were $N = 0.21$ and $E/K = 124.0$ as given in [5] in order to compare predicted results with existing test data for aluminum specimens. For the computations simulating rate-sensitivity effects we took $\kappa = 0.018$ and $\dot{\epsilon}_R = 0.000137/s$ as given in [16]. These values were determined experimentally for A–K steel ($N = 0.22$) and should be typical of other metals at room temperature. The constant ϵ_0 in (3.19) was determined by setting the yield strain $\epsilon_y = 0.001$ and imposing continuity of σ_u at yield. The material parameters varied in this study were the anisotropic yield function constants n, m and R in (3.11).

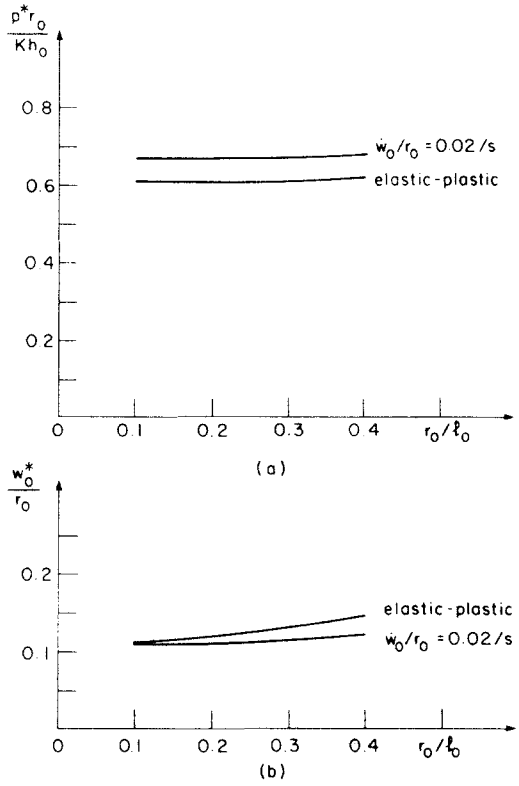

Fig. 4. Dependence of maximum pressure p^* and corresponding deflections w_0^* on diameter-to-length ratio of tube for both rate-sensitive and time-independent behaviour.

Table 1. Influence of tube geometry on stress ratio σ_z/σ_θ according to flow theory

$r_0/\ell_0 = 0.1$		$r_0/\ell_0 = 0.2$		$r_0/\ell_0 = 0.3$		$r_0/\ell_0 = 0.4$	
w_0/r_0	σ_z/σ_θ	w_0/r_0	σ_z/σ_θ	w_0/r_0	σ_z/σ_θ	w_0/r_0	σ_z/σ_θ
$0.2\ 10^{-3}$	0.500	$0.1\ 10^{-4}$	0.500	$0.2\ 10^{-3}$	0.500	$0.2\ 10^{-3}$	0.500
$0.1\ 10^{-2}$	0.500	$0.5\ 10^{-3}$	0.500	$0.4\ 10^{-3}$	0.500	$0.9\ 10^{-3}$	0.500
0.021	0.500	0.021	0.500	0.021	0.504	0.021	0.506
0.061	0.500	0.041	0.500	0.041	0.506	0.041	0.509
0.101	0.500	0.061	0.500	0.081	0.509	0.061	0.512
0.113	0.500	0.081	0.500	0.101	0.511	0.081	0.516
		0.101	0.505	0.121	0.514	0.101	0.520
		0.121	0.506	0.131	0.516	0.121	0.526
						0.141	0.533
						0.144	0.534

Table 2. Influence of tube geometry on stress ratio σ_z/σ_θ according to deformation theory

$r_0/\ell_0 = 0.1$		$r_0/\ell_0 = 0.2$		$r_0/\ell_0 = 0.3$		$r_0/\ell_0 = 0.4$	
w_0/r_0	σ_z/σ_θ	w_0/r_0	σ_z/σ_θ	w_0/r_0	σ_z/σ_θ	w_0/r_0	σ_z/σ_θ
$0.2\ 10^{-3}$	0.500	$0.1\ 10^{-4}$	0.500	$0.2\ 10^{-3}$	0.500	$0.2\ 10^{-3}$	0.500
$0.1\ 10^{-2}$	0.500	$0.5\ 10^{-3}$	0.500	$0.4\ 10^{-3}$	0.500	$0.9\ 10^{-3}$	0.500
0.021	0.500	0.021	0.500	0.021	0.501	0.021	0.501
0.061	0.500	0.041	0.500	0.041	0.501	0.041	0.502
0.101	0.500	0.061	0.500	0.081	0.503	0.061	0.504
0.113	0.500	0.081	0.500	0.101	0.505	0.081	0.506
		0.101	0.502	0.121	0.507	0.101	0.509
		0.121	0.503	0.131	0.508	0.121	0.513
						0.141	0.517
						0.144	0.518

Table 3. Influence of tube geometry on parameter $\sigma_\theta h/p(r_0 + w_0)$ according to flow theory

$r_0/\ell_0 = 0.1$		$r_0/\ell_0 = 0.2$		$r_0/\ell_0 = 0.3$		$r_0/\ell_0 = 0.4$	
w_0/r_0	$\frac{\sigma_\theta h}{p(r_0 w_0)}$	w_0/r_0	$\frac{\sigma_\theta h}{p(r_0+w_0)}$	w_0/r_0	$\frac{\sigma_\theta h}{p(r_0+w_0)}$	w_0/r_0	$\frac{\sigma_\theta h}{p(r_0+w_0)}$
$0.2\ 10^{-3}$	1.000	$0.1\ 10^{-4}$	1.000	$0.2\ 10^{-3}$	1.000	$0.2\ 10^{-3}$	1.000
$0.1\ 10^{-2}$	1.000	$0.5\ 10^{-3}$	1.000	$0.4\ 10^{-3}$	1.000	$0.9\ 10^{-3}$	1.000
0.021	1.000	0.021	1.000	0.021	1.000	0.021	1.000
0.061	1.000	0.041	1.000	0.041	1.000	0.041	0.998
0.101	1.000	0.061	1.000	0.081	0.997	0.061	0.996
0.113	1.000	0.081	0.998	0.101	0.994	0.081	0.993
		0.101	0.997	0.121	0.990	0.101	0.988
		0.121	0.995	0.131	0.987	0.121	0.981
						0.141	0.973
						0.144	0.972

Results for time-independent, isotropic behaviour ($n = m = 2$, $R = 1$) are first shown in Fig. 2 where the maximum pressure p^* and corresponding expansion level w_0^* are given in terms of the diameter-to-length ratio r_0/l_0 of the tube. Solid curves here represent the numerical results obtained from the finite element calculations. The flow theory and deformation theory curves are indistinguishable in these figures. Squares in Fig. 2 refer to the experimental data of Banerjee[5], while the open circles correspond to the approximate formulae (5–6). An excellent agreement between the theoretical predictions and experimental results is obtained, especially for the longer tubes ($r_0/l_0 \leq 0.2$). For the shorter tubes ($r_0/l_0 = 0.4$) the predicted maximum pressures are somewhat lower than the test results. These discrepancies in the short-tube range are most likely due to bending effects, which are neglected in the analysis. Figure 2 also shows that the approximate analysis of Section 5 and finite element calculations give virtually identical predictions for tubes with length-to-diameter ratios greater than about 10.

A comparison between the finite element results and those obtained assuming a uniform expansion of the tube is given in Tables 1–4 for isotropic tubes with various geometries. Rate-independent behaviour is again considered here. According to the long-tube relations we have $\sigma_z/\sigma_\theta = 1/2$ and

Table 4. Influence of tube geometry on parameter $\sigma_\theta h/p(r_0 + w_0)$ according to deformation theory

$r_0/\ell_0 = 0.1$		$r_0/\ell_0 = 0.2$		$r_0/\ell_0 = 0.3$		$r_0/\ell_0 = 0.4$	
w_0/r_0	$\frac{\sigma_\theta h}{p(r_0+w_0)}$	w_0/r_0	$\frac{\sigma_\theta h}{p(r_0+w_0)}$	w_0/r_0	$\frac{\sigma_\theta h}{p(r_0+w_0)}$	w_0/r_0	$\frac{\sigma_\theta h}{p(r_0+w_0)}$
$0.2\ 10^{-3}$	1.000	$0.1\ 10^{-4}$	1.000	$0.2\ 10^{-3}$	1.000	$0.2\ 10^{-3}$	1.000
$0.1\ 10^{-2}$	1.000	$0.5\ 10^{-3}$	1.000	$0.4\ 10^{-3}$	1.000	$0.9\ 10^{-3}$	1.000
0.021	1.000	0.021	1.000	0.021	1.000	0.021	1.000
0.061	1.000	0.041	1.000	0.041	1.000	0.041	0.998
0.101	1.000	0.061	1.000	0.081	0.997	0.061	0.996
0.113	1.000	0.081	0.998	0.101	0.994	0.081	0.993
		0.101	0.997	0.121	0.990	0.101	0.988
		0.121	0.995	0.131	0.987	0.121	0.982
						0.141	0.974
						0.144	0.973

$$\frac{\sigma_\theta h}{p(r_0 + w_0)} = 1 \tag{6.2}$$

Values of the stress ratio σ_z/σ_θ at $z = 0$, obtained with flow theory and deformation theory are listed in Tables 1 and 2, respectively, while values of the parameter defined by eqn (6.2) are given in Tables 3 and 4. Again, we observe an almost perfect agreement between the approximate and exact numerical results for long tubes ($r_0/l_0 = 0.1$), even for expansions up to about 12% of the tube radius. The approximate formulae lose accuracy as the tube becomes shorter because of the increasing importance of end effects. The discrepancies, however, remain relatively small and are slightly less with deformation theory than with flow theory.

The last lines in Tables 1–4 correspond to the maximum pressure state. According to (5.6) this occurs at an expansion $w_0^*/r_0 = 0.111$ which is quite close to the value ($w_0^*/r_0 = 0.113$) obtained for the long tube. Furthermore, eqn (5.7) indicates that localized necking takes place when $w_0^{(l)}/r_0 = 0.234$. The corresponding result obtained by incorporating a bifurcation criterion in the deformation theory finite element calculations for $r_0/l_0 = 0.1$ is $w_0^{(l)}/r_0 = 0.228$.

The influence of the anisotropic parameters n, m and R on the maximum pressure p^* is depicted in Fig. 3. Time-independent behaviour is assumed, and long tubes are considered. Equation (5.6c) gives essentially the same curves as those predicted numerically with flow theory and deformation theory. Figure 3 shows that the maximum pressure increases substantially with increasing R and decreasing n. However, as indicated by (5.6b), the corresponding expansion level w_0^* is independent of the anisotropic parameters; it depends only on the strain-hardening exponent N.

The influence of material strain-rate sensitivity is shown in Fig. 4. Here the maximum pressure and corresponding deflection are plotted as a function of the tube diameter-to-length ratio. The lower curves correspond to time-independent behaviour ($\kappa = 0$) while the upper curves represent rate-dependent (viscoplastic) response. An expansion rate $\dot{w}_0/r_0 = 0.02/s$ was prescribed for the time-dependent calculations. As seen in Fig. 4(a), rate-sensitivity leads to an increase in the maximum pressure over its time-independent values. The amount of increase is practically constant over the range of tube geometries considered. Figure 4(b) indicates that rate-sensitivity has a much less effect on the deflection w_0^* at maximum pressure and that the effect decreases as the tube length increases. For long tubes rate-dependence has no noticeable influence on the value of w_0^*, as suggested by (5.9).

From the present study we can conclude that, for internally-pressurized thin-walled cylinders, the simplified formulae commonly used to treat experimental data are extremely accurate if the length-to-diameter ratio is sufficiently large ($l_0/r_0 = 5$–10). End effects, however, are not negligible for shorter tubes. For long cylinders eqns (5.5)–(5.9) appear to be sufficiently accurate for determining the influence of material properties (including anisotropy) on the pressure-deformation response and instabilities in thin tubes. The present investigation also indicates that both material anisotropy and strain-rate sensitivity can significantly influence the maximum pressure which a fixed-end tube can sustain. However, the corresponding expansion level at the maximum pressure is virtually insensitive to anisotropy and rate-dependent effects. Finally, we note that no significant differences are observed between the predictions of flow theory and deformation theory for the overall pressure-expansion behaviour of the cylinder.

Acknowledgements—This work was supported by the Natural Sciences and Engineering Research Council of Canada (Grant A-8584) and by le Ministère de l'éducation du Québec (Programme FCAC).

REFERENCES

1. N. A. Weil, Tensile instability of thin walled cylinders of finite length. *Int. J. Mech. Sci.* **5**, 487–506 (1963).
2. P. Mann-Nachbar, O. Hoffman and W. E. Jahsman, Plastic instability of cylindrical pressure vessels of finite length. *AIAA J.* **1**, 1607–1613 (1967).
3. M. A. Salmon, Plastic instability of cylindrical shells with rigid end closures. *J. Appl. Mech.* **30**, 401–409 (1963).
4. M. A. Salmon, Large plastic deformation of pressurized cylinders. *J. Engng Mech. Div. ASCE* **92**, 33–51 (1966).
5. J. K. Banerjee, Limiting deformations in bulge forming of thin cylinders of fixed length. *Int. J. Mech. Sci.* **17**, 659–662 (1975).
6. R. Hill, *The Mathematical Theory of Plasticity*. Oxford University Press (1950).
7. R. Hill, Theoretical plasticity of textured aggregates. *Math. Proc. Camb. Phil. Soc.* **85**, 179–191 (1979).
8. J. L. Bassani, Yield characterization of metals with transversely isotropic plastic properties. *Int. J. Mech. Sci.* **19**, 651–660 (1977).
9. B. Budiansky, Anisotropic plasticity of plane-isotropic sheets. Harvard University Rep. Mech-26 (March 1982).
10. R. Hill, Uniqueness criteria and extremum principles in self-adjoint problems of continuum mechanics. *J. Mech. Phys. Solids* **10**, 185–194 (1962).
11. E. Chater and K. W. Neale, Finite plastic deformation of a circular membrane under hydrostatic pressure—II. Strain-rate effects. *Int. J. Mech. Sci.*, to be published.
12. J. W. Hutchinson, Finite strain analysis of elastic–plastic solids and structures. In *Numerical Solution of Nonlinear Structural Porblems* (Edited by R. F. Hartung), pp. 17–29. ASME (1973).
13. M. J. Sewell, On configuration-dependent loading. *Arch. Rat. Mech. Anal.* **23**, 327–351 (1967).
14. J. W. Hutchinson and K. W. Neale, Sheet necking—III. Strain-rate effects. In *Mechanics of Sheet Metal Forming* (Edited by D. P. Koistinen and N. M. Wang), pp. 269–285. Plenum Press, New York (1978).
15. K. W. Neale and E. Chater, Limit strain predictions for strain-rate sensitive anisotropic sheets. *Int. J. Mech. Sci.* **22**, 563–574 (1980).
16. N. M. Wang and M. L. Wenner, Elastic–viscoplastic analyses of simple stretch forming problems. In *Mechanics of Sheet Metal Forming* (Edited by D. P. Koistinen and N. M. Wang), pp. 367–398. Plenum Press, New York (1978).
17. E. Chater and K. W. Neale, A finite element method for large-strain plasticity problems. *Proc. 10th IMACS World Congress on System Simulation and Scientific Computation*, Montréal, Canada, 1982 (Edited by W. F. Ames and R. Vichnevetsky). North Holland, Amsterdam, to be published.

APPENDIX

The instantaneous compliances in (4.9) for time-independent behaviour are obtained from (3.1) and (3.5) for flow theory. Equation (3.1) together with the rate form of (3.8) give the deformation theory compliances. For flow theory we get

$$M_{zz}^{(F)} = \frac{1}{E} + \left(\frac{\partial \sigma_u}{\partial \sigma_z}\right)^2 \left(\frac{1}{E_t} - \frac{1}{E}\right)$$

$$M_{z\theta}^{(F)} = -\frac{1}{2E} + \left(\frac{\partial \sigma_u}{\partial \sigma_z}\right)\left(\frac{\partial \sigma_u}{\partial \sigma_\theta}\right)\left(\frac{1}{E_t} - \frac{1}{E}\right) \tag{A1}$$

$$M_{\theta\theta}^{(F)} = \frac{1}{E} + \left(\frac{\partial \sigma_u}{\partial \sigma_\theta}\right)^2 \left(\frac{1}{E_t} - \frac{1}{E}\right)$$

while deformation theory gives

$$M_{zz}^{(D)} = M_{zz}^{(F)} - \sigma_u \frac{\partial^2 \sigma_u}{\partial \sigma_z^2}\left(\frac{1}{E_s} - \frac{1}{E}\right)$$

$$M_{z\theta}^{(D)} = M_{z\theta}^{(F)} + \sigma_u \frac{\partial^2 \sigma_u}{\partial \sigma_z \partial \sigma_\theta}\left(\frac{1}{E_s} - \frac{1}{E}\right) \tag{A2}$$

$$M_{\theta\theta}^{(D)} = M_{\theta\theta}^{(F)} + \sigma_u \frac{\partial^2 \sigma_u}{\partial \sigma_\theta^2}\left(\frac{1}{E_s} - \frac{1}{E}\right).$$

The instantaneous compliances in (4.11) for strain-rate sensitive behaviour are the elastic compliances for flow theory, and are obtained from (3.18) with deformation theory. Thus, for flow theory we have

$$M_{zz}'^{(F)} = M_{\theta\theta}'^{(F)} = \frac{1}{E}$$

$$M_{z\theta}'^{(F)} = -\frac{1}{2E}. \tag{A3}$$

Deformation theory gives

$$M_{zz}'^{(D)} = M_{zz}'^{(F)} + \epsilon_u^{vP} \frac{\partial^2 \sigma_u}{\partial \sigma_z^2}$$

$$M_{z\theta}'^{(D)} = M_{z\theta}'^{(F)} + \epsilon_u^{vP} \frac{\partial^2 \sigma_u}{\partial \sigma_z \partial \sigma_\theta} \tag{A4}$$

$$M_{\theta\theta}'^{(D)} = M_{\theta\theta}'^{(F)} + \epsilon_u^{vP} \frac{\partial^2 \sigma_u}{\partial \sigma_\theta^2}.$$